

# Longitudinal Multimodal fMRI to Investigate Neurovascular Changes in Spontaneously Hypertensive Rats

Andrew Crofts, Melissa Trotman-Lucas, Justyna Janus, Michael Kelly, and Claire L. Gibson 

From the Department of Neuroscience, Psychology & Behaviour, University of Leicester, Leicester, UK (AC, MTL, CLG); School of Psychology, University of Nottingham, Nottingham, UK (MTL, CJG); and Preclinical Imaging Facility, Core Biotechnology Services, University of Leicester, Leicester, UK (AC, JJ, MK).

## ABSTRACT

Hypertension is an important risk factor for age-related cognitive decline and neuronal pathologies. Studies have shown a correlation between hypertension, disruption in neurovascular coupling and cerebral autoregulation, and cognitive decline. However, the mechanisms behind this are unclear. To further understand this, it is advantageous to study neurovascular coupling as hypertension progresses in a rodent model. Here, we use a longitudinal functional MRI (fMRI) protocol to assess the impact of hypertension on neurovascular coupling in spontaneously hypertensive rats (SHRs). Eight female SHRs were studied at 2, 4, and 6 months of age, as hypertension progressed. Under an IV infusion of propofol, animals underwent fMRI, functional MR spectroscopy, and cerebral blood flow (CBF) quantification to study changes in neurovascular coupling over time. Blood pressure significantly increased at 4 and 6 months ( $P < .0001$ ). CBF significantly increased at 4 months old ( $P < .05$ ), in the acute stage of hypertension. The size of the active region decreased significantly at 6 months old ( $P < .05$ ). Change in glutamate signal during activation, and N-acetyl-aspartate (NAA) signal, remained constant. This study shows that, while cerebral autoregulation is impaired in acute hypertension, the blood oxygenation-level-dependent (BOLD) response remains unaltered until later stages. At this stage, the consistent NAA and glutamate signals show that neuronal death has not occurred, and that neuronal activity is not affected at this stage. This suggests that neuronal activity and viability is not lost until much later, and changes observed here in BOLD activity are due to vascular effects.

**Keywords:** Hypertension, fMRI, neurovascular coupling, cerebral blood flow, MRS.

**Acceptance:** Received June 3, 2020, and in revised form June 22, 2020. Accepted for publication June 23, 2020.

**Correspondence:** Address correspondence to Professor Claire L. Gibson, School of Psychology, University of Nottingham, University Park, Nottingham NG7 2UH, UK. E-mail: [claire.gibson@nottingham.ac.uk](mailto:claire.gibson@nottingham.ac.uk)

**Acknowledgments and Disclosure:** A.C. is supported by Medical Research Council IMPACT DTP PhD Studentship (grant number MR/N013913/1). The authors have no competing interests related to the study.

J Neuroimaging 2020;00:1-8.

DOI: 10.1111/jon.12753

## Introduction

In recent decades, evidence has shown a role for the vascular system in age-related cognitive decline and age-related neurodegeneration.<sup>1</sup> Hypertension is now widely accepted as a risk factor for cognitive decline and neurodegenerative disease.<sup>2</sup> Functional MRI (fMRI) studies in humans have shown impaired cerebral blood flow (CBF) and diminished blood oxygenation-level-dependent (BOLD) response in a number of brain regions in hypertensive subjects, as well as disruption to functional connectivity.<sup>3</sup> The mechanisms behind these changes in neurovascular coupling are currently unclear, although are thought to begin as adaptive responses to acute hypertension, which are protective in the short term. However, in chronic hypertension, these changes are thought to cause impairments in functional hyperemia in the long term, leading to hypoxia in neurons, contributing to factors, such as oxidative damage.<sup>4</sup> As rodent models of hypertension exist,<sup>5</sup> it is possible to apply longitudinal fMRI methods to reveal how vascular changes correlate with changes in neuronal activity as hypertension progresses.

Arterioles and capillaries exhibit adaptation to acute hypertension shortly after onset, and these adaptations are thought to maintain cerebral autoregulation and be neuroprotective in the

short term. The initial phase of remodeling, eutrophic remodeling, is thought to improve the vessel wall's resistance to stress and reduce CBF to healthy levels for short periods of time.<sup>6</sup> This phase does not include an increase in the mass of smooth muscle or pericytes, and is reversible if hypertension is resolved. In chronic hypertension, permanent changes occur due to hypertrophic remodeling, in which smooth muscle and pericytes grow thicker due to collagen deposition. While this prevents damage from increased stress and reduces CBF, this increased thickness reduces vascular reactivity and functional hyperemia, as well as blood-brain barrier permeability.<sup>7</sup>

Such changes are reflected in human imaging studies where hypertension has been shown to affect task-related BOLD response, and genetic risk of hypertension has been shown to have an impact on the cognitive and neurovascular function even before symptomatic onset.<sup>8-10</sup> For example, normotensive patients with family history of hypertension showed a significant decrease in BOLD signal intensity in three cognitive regions during a visuospatial task, compared to controls with no history of hypertension.<sup>10</sup> However, another study showed increased BOLD signal in middle-aged hypertensive patients in multiple regions during a cognitive task, and recruited additional cortical regions not observed in controls.<sup>11</sup>

This is an open access article under the terms of the Creative Commons Attribution License, which permits use, distribution and reproduction in any medium, provided the original work is properly cited.

Other MRI outcome measures also been shown to be affected by hypertension include increases and decreases in functional connectivity between certain areas correlated with impaired performance in verbal cognitive tasks.<sup>12</sup> This suggests a combination of pathological changes, where connectivity is impaired, and compensatory changes where connectivity is increased, within the same cohort as hypertension progresses. This is also supported by CBF imaging, showing impaired CBF in the right cortex, with compensatory increases in CBF in the left cortex.<sup>3</sup> Cerebral glucose uptake is also impaired in the hippocampus and in cortical regions connecting to the hippocampus involved in spatial learning.<sup>13</sup> Thus, a longitudinal preclinical study of progressive hypertension can improve understanding of the multiple compensatory and pathological changes that occur.

In this study, we used an MRI protocol investigating the BOLD signal, resting CBF, changes in metabolite and neurotransmitter levels, and functional connectivity to study the effects of progressive hypertension in spontaneously hypertensive rats (SHRs) from 2 months old (normotensive) to 6 months old (chronic hypertension). SHRs are a strain bred from the Wistar Kyoto rat to select for high blood pressure (BP), which are normotensive for the first 6-8 weeks of life, and then develop hypertension between 2 and 5 months old.<sup>14</sup> Changes to neuronal and vascular activity as hypertension progresses were investigated using a minimally invasive anesthetic protocol and a longitudinal study design.<sup>15</sup>

## Methods

### *Animals*

This study was conducted in accordance with the UK Animals (Scientific Procedures) Act, 1986 and following ethical approval by the University of Leicester Animal and Welfare Ethical Review Body. All experiments are reported in accordance with the Animal Research Reporting of In Vivo Experiments (ARRIVE) guidelines.<sup>16</sup> A total of eight female SHRs (NHsd, Ennigo, Shardlow, Derbyshire, UK) aged 3 weeks on arrival were housed in double decker cages (floor area 1,862 cm<sup>2</sup>, height 38 cm, Techniplast, UK) in two groups of four animals. Animals were given daily access to a playpen for 2-6 hours. Assuming an effect size of 35%, based on CBF fMRI in normotensive and hypertensive humans,<sup>3</sup> power calculations suggested eight animals to be sufficient to observe this effect across three time points. Animals were fed PMI 5LF2 diet (Lab Supply, Fort Worth, TX) ad libitum and mains water that had been ultraviolet (UV) treated in house (Severn Trent, UK).

### *Experimental Schedule*

After a week of acclimatization to the animal unit, animals were acclimatized to the playpen in groups of 4 over 2 days, before putting the entire cohort into one playpen from day 3 onward. For 1 week, animals were acclimatized to the BP monitoring equipment, and BP was then taken weekly for the duration of the study. Animals were weighed prior to all MRI scans. The first MRI scan was performed between 6 weeks and 2 months of age, prior to the onset of hypertension, and subsequent scans were performed at 4 and 6 months of age. Immediately following the final scan, animals were humanely killed using intraperitoneal pentobarbitone and transcardially perfused with formaldehyde.

### *BP Monitoring*

BP was taken using a Kent Scientific Coda 4.1 BP monitoring system (Kent Scientific Corporation, Torrington, CT). Animals were trained to enter a plastic tube, after which they were sealed in with a nose cone at one end and cover with a tail hole at the other. The nose cone was adjusted to prevent the rat turning around but not to cause discomfort. Two cuffs were placed over the tail, the occlusion cuff at the base and the detection cuff at the tip. Fifteen averages were taken, with the first five discarded as acclimatization to the system, and any averages with motion artifacts discarded.

### *Anesthesia Protocol*

This study uses an anesthesia propofol initially described by Griffin et al,<sup>17</sup> which we have implemented and refined.<sup>15</sup> Animals were anesthetized with isoflurane (5% induction; 2-3% maintenance) in 100% oxygen. Tail vein cannulation was performed before transferring the animals to the MRI cradle. A bolus of 9 mg/kg/min propofol was administered for 1 minute using a syringe driver (Harvard Apparatus, Cambridge, MA) and the isoflurane was gradually reduced to 0%, with animals still breathing 100% oxygen. Respiration was monitored using a respiration pillow (Small Animal Instruments Inc., Stony Brook, NY), temperature monitored using a rectal probe and maintained using a fan heater activated when measured temperature dropped below 37 °C (Small Animal Instruments Inc.), and heart rate and blood oxygen saturation monitored using a pulse oximeter (Starr Life Sciences, Oakmont, PA). Copper electrodes were inserted subcutaneously into the dorsal surface of the right forepaw between digits 1-2 and 2-3.<sup>18</sup> Three minutes after the bolus ended, a continuous infusion of propofol was given at 54 mg/kg/h until fMRI and fMRS were completed, and animals were switched to breathing room air. For the duration of the time-of-flight (TOF) angiography, T2 weighted structural scan, and arterial spin labeling (ASL) scan, animals were given 1.5% isoflurane in 100% oxygen. Following the scan, animals were allowed to recover in a separate cage. Analgesic cream (EMLA cream, AstraZeneca, UK) was applied to the forepaw where electrodes had been removed, and animals were provided with water and wet food pellets to prevent dehydration after anesthesia. Animals were awake within 15 minutes following the removal of anesthesia, and moving freely within 30 minutes, at which point they were returned to their home cages.

### *MRI Protocol*

This study used an MRI protocol adapted from the multiparametric MRI protocol, which we have previously implemented in healthy, aging rats.<sup>15</sup> MRI scans were performed on a 9.4T Small Animal MRI scanner (Agilent Technologies), using a 72 mm RF volume transmit coil and a 2-channel surface receive coil (Rapid Biomedical, Rimpar, Germany). Coronal scout images were used to locate bregma, and three 1.5 mm slices were selected with bregma in the middle slice. A shimming voxel with dimensions 10 × 9 × 4.5 mm was positioned to cover the center of all three slices, excluding nonbrain tissue or tissue outside the slices of interest. Fast, automatic shimming technique by mapping along projections (FASTMAP)<sup>19</sup> was used to shim these slices to a 50% water linewidth between 20 and 35 Hz. Rats were switched from breathing oxygen to room air, pumped

at 2 L/min using an air pump (Wiz-Air, Clarke Tools, Dunstable, UK). fMRI was performed for 9 minutes using a gradient echo EPI sequence (TR = 250 milliseconds, TE = 22 milliseconds, kzero = 8, shots = 2, data matrix = 128 × 128). The forepaw was stimulated at 10 mV, 10 Hz, and pulse width 1  $\mu$ s, which has previously been confirmed to activate somatosensory fibers without activating nociceptive fibers.<sup>17</sup> The stimulus paradigm used a block design of 60 seconds off and 30 seconds on. Following this, a 4 × 4 × 4 mm voxel was positioned over the left primary somatosensory cortex, forepaw region (S1FL) at bregma, and manual shimming was performed to a 50% water linewidth of <25 Hz. A localization by adiabatic selective refocusing (LASER)<sup>20</sup> MRS sequence (TR = 2,000 milliseconds, TE = 14.54 milliseconds, and 270 arrayed averages) was used to perform fMRS over 18 minutes, using the same forepaw stimulation paradigm used for fMRI. For analysis, the first 30 seconds of each “off” block were discarded to allow time for metabolites to return to baseline levels. Oxygen saturation was maintained above 80% during functional experiments.<sup>21</sup> Animals were switched back to 100% oxygen and 1.5% isoflurane after all functional scans were complete, to prevent the risk of the animal waking up as lidocaine wore off and the tail vein constricted. After being returned to 100% oxygen, a TOF angiography scan was performed in order to locate a labeling plane for ASL, followed by a T2 weighted structural scan. Using the TOF angiography image, the carotid artery was located and a labeling plane placed with a gap of -17 mm from bregma. Six minutes of continuous arterial spin labeling was performed on a single 1.5 mm slice placed over bregma (TI = 1,500 milliseconds, TR = 2,500 milliseconds, TE = 10 milliseconds, shots = 1, kzero = 16, and data matrix = 128 × 128).

### Data Analysis

An fMRI analysis pipeline was performed using the FMRIB software library (FSL [www.fmrib.ox.ac.uk/fsl](http://www.fmrib.ox.ac.uk/fsl)).<sup>22</sup> Motion correction with FMRIB’s linear registration tool (MCFLIRT),<sup>23</sup> the rat brain extraction tool (rBET, a modified version of BET to account for the different shape of the rat brain compared to humans),<sup>24,25</sup> and FMRIB’s automated segmentation tool (FAST)<sup>26</sup> was used for motion correction, brain extraction, and bias field correction, respectively. Independent component analysis for artifact removal, using multivariate exploratory linear optimized decomposition into independent components (MELODIC),<sup>27</sup> was performed prior to time-series analysis in FMRIB’s expert analysis tool (FEAT)<sup>28</sup> to visualize the BOLD response. Cluster analysis was performed on the first-level FEAT outputs to determine the number of active voxels, maximum % signal change within the cluster, and mean % signal change across the cluster. In each scan, time to peak was calculated for each of the six stimulus blocks and averaged, with a temporal resolution of .5 seconds.<sup>29</sup>

fMRS spectra were separated into “off” and “on” blocks and averaged using the MATLAB FID-A toolkit.<sup>30</sup> The two spectra were analyzed using the TARQUIN MRS analysis package ([www.tarquin.sourceforge.net](http://www.tarquin.sourceforge.net)) to determine relative concentrations of glutamate. Metabolite concentrations from “off” blocks were subtracted from “on” blocks to determine the difference in glutamate concentration, and the difference in glutamate change ( $\Delta$ Glu) was averaged across subjects. “Off” blocks were also used to quantify N-acetyl-aspartate (NAA) and inos-

itol, used as markers of neuronal viability and inflammation, respectively.

Control and tag ASL images were first concatenated into a single image of two volumes. The Oxford ASL toolkit for FSL was used to subtract the tag image from the control image to create a difference image. FSLmaths was used to apply a modified Bloch equation<sup>31</sup> to the data in order to quantify CBF in absolute units. CBF map images were given an upper threshold of 5 to remove large outliers. This was determined based on the histogram of voxel intensities, in which some scans displayed a small number of single voxels with large intensities between 5 and 80 having a large influence on the mean. Nonzero mean and standard deviation CBF were calculated using FSLstats.

Statistical analysis was performed in Graphpad Prism (Version 8, La Jolla, CA). Data are shown as mean  $\pm$  standard deviation (SD). Changes over time were analyzed using a repeated measures ANOVA, fitting a mixed effects model to account for missing values, and the criterion for statistical significance was  $P < .05$ . Where statistically significant differences were found, post-hoc testing to compare individual time points was performed using the Tukey-Kramer multiple comparisons test.

## Results

### BP and Body Weight

Mean body weight increased over time from 123.0  $\pm$  6.78 g at 2 months old to 201.5  $\pm$  19.7 g at 6 months ( $F(2, 14) = 62.55$ ,  $P < .0001$ , Fig 1A). Animals showed a consistent increase in systolic ( $F(2,452) = 148.4$ ,  $P < .0001$ ) and diastolic ( $F(2,452) = 109.2$ ,  $P < .0001$ ) BP over the duration of the study (Fig 1B and C). Systolic BP increased 28% between 2 and 4 months ( $P < .0001$ ), and increased 11% between 4 and 6 months ( $P < .0001$ ). Diastolic BP increased 22% between 2 and 4 months ( $P < .0001$ ), and increased 27% between 4 and 6 months ( $P < .0001$ ). Pulse pressure changed significantly over time ( $F(2, 452) = 15.0$ ,  $P < .0001$ ), increasing by 61% between 2 and 4 months ( $P < .0001$ ), and decreasing by 49% between 4 and 6 months ( $P < .0001$ , Fig 1D).

### BOLD fMRI

Analysis of BOLD fMRI data was performed in FEAT (Fig 2) and was used to quantify three aspects of the BOLD signal: number of active voxels in S1FL, maximum % signal change in S1FL, and mean % signal change in S1FL (Fig 3). The number of active voxels in S1FL significantly decreased over time ( $F(2, 16) = 4.834$ ,  $P = .0228$ ) with post-hoc testing showing a significant decrease between 4 and 6 months from 71  $\pm$  32 voxels to 29  $\pm$  26 voxels ( $P = .0254$ ). Maximum and mean % BOLD signal change showed no significant change over time (Max  $F(2, 16) = 2.139$ ,  $P = .1502$ . Mean  $F(2, 16) = 2.827$ ,  $P = .0888$ ).

### Functional MR Spectroscopy

At the first time point measured (2 months), mean glutamate change with activation ( $\Delta$ Glu) was .99645 + 1.69. No significant change was observed over time ( $F(2, 11) = 1.317$ ,  $P = .3071$ , Fig 4A). Analysis was also performed on the NAA signal, which was 1.58  $\pm$  2 at 2 months and did not change significantly over time ( $F(2, 14) = 1.086$ ,  $P = .3642$ , Fig 4B).

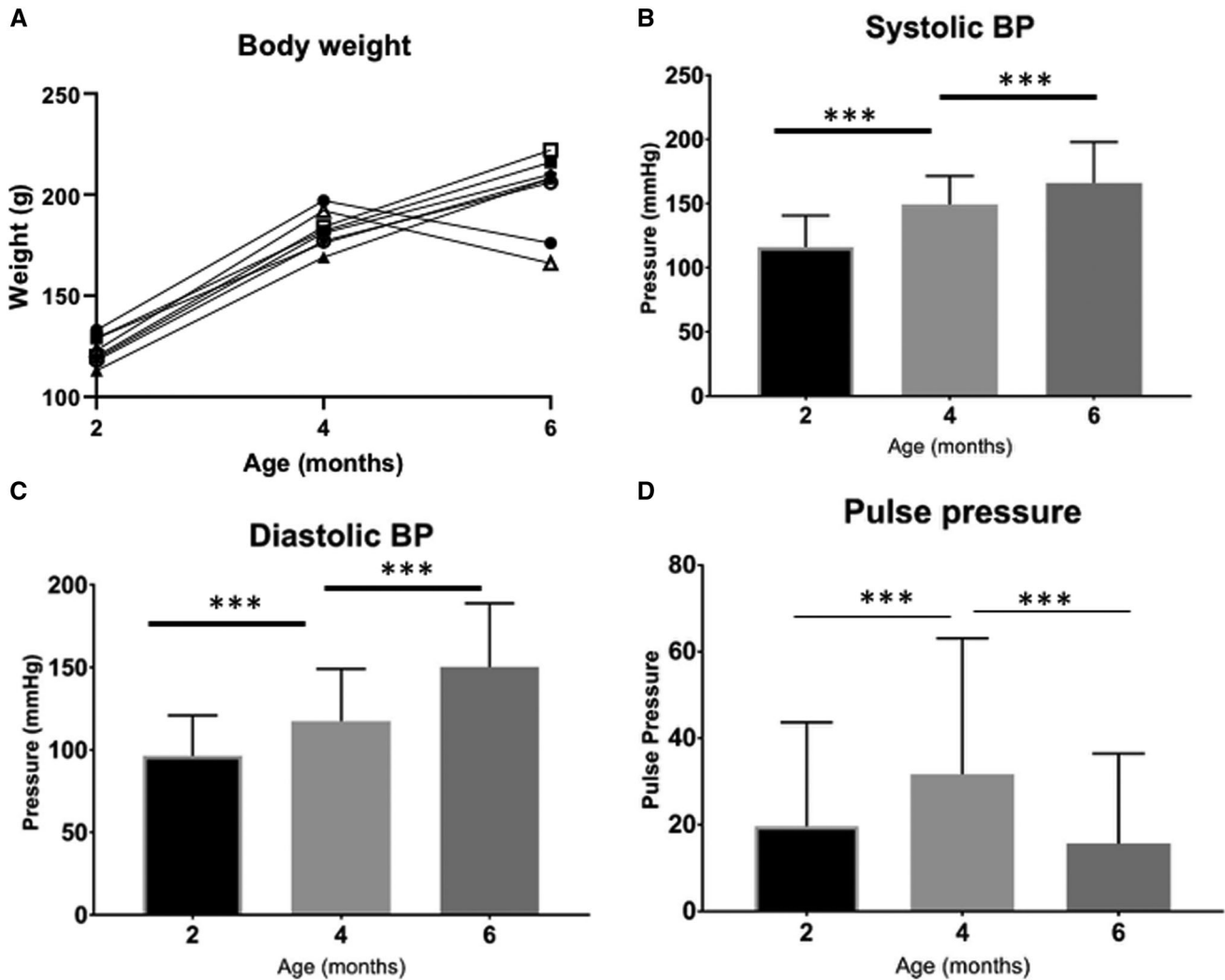


**Fig 1.** Individual rat weights at 2, 4, and 6 months of age (A). Mean rat systolic blood pressure (B), diastolic blood pressure (C), and pulse pressure (D) at 2, 4, and 6 months of age (Number = 8). \*\*\* =  $P < .0001$

### Arterial Spin Labeling

Mean CBF significantly changed over time ( $F(2, 18) = 8.738$ ,  $P = .017$ , Fig 5). Post-hoc testing showed a significant increase from  $1.616 \pm .253$  mL/mg/min at 2 months old to  $2.422 \pm .486$  at 4 months old ( $P = .0285$ ). CBF at 6 months was also significantly greater than 2 months ( $P = .0110$ ).

### Discussion

This study used fMRI to observe, for the first time, changes in the BOLD signal and CBF over time in SHR, as animals progressed from normotension to chronic hypertension. This study also observed glutamate turnover and NAA levels in SHR for the first time. Propofol was determined to be a suitable anesthetic for the detection of the BOLD signal, and with no detrimental effects on animal health, as we have previously found in healthy aging animals.<sup>15</sup> BP increased significantly between each time point. Systolic BP and diastolic BP increased at different rates, causing pulse pressure to increase between 2 and 4 months and return to baseline between 4 and 6 months. This change in BP correlated with previous measurements of SHR.<sup>14</sup> The size of the BOLD signal in S1FL increased be-

tween 2 and 4 months and also returned to baseline between 4 and 6 months. CBF increased between 2 and 4 months, and remained high at 6 months old. Functional MR spectroscopy showed no significant change in glutamate turnover. We chose 6 months as a humane end point for this study, as the survival rate for SHR at 6 months old is 98%,<sup>32</sup> and before any other health problems, such as kidney failure, may present, which could produce ill effects in combination with the anesthetic.

In the acute stage of hypertension, ie, ~4 months in SHR,<sup>14,32</sup> adaptive changes are thought to occur in the brain's vasculature.<sup>11,13</sup> As the BOLD response is not significantly altered at the 4 month time point, when pulse pressure is the highest, these adaptations may be linked to pulse pressure rather than the increased systolic BP. The decrease in pulse pressure, as diastolic BP increases more rapidly, may then be the point in which adaptive changes to the vascular become pathological. Previous studies suggest that SHR have been shown to favor eutrophic remodeling, rather than hypertrophic remodeling. In eutrophic remodeling, muscle in the arteries rearranges to narrow the lumen, and in hypertrophic remodeling, growth of new smooth muscle and perivascular cells occurs. These results suggest that eutrophic remodeling may occur in the acute



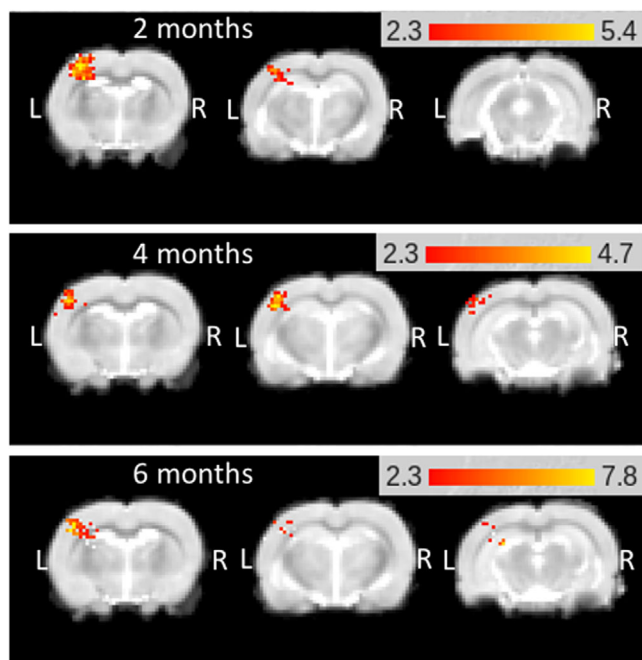


**Fig 2.** Example images displaying primary somatosensory cortex, forepaw region activation in a representative rat.

stage, to preserve vascular reactivity, while hypertrophic remodeling occurs in the chronic stage and decreases reactivity, which is thought to be how hypertension progresses in humans.<sup>6,7</sup>

It is important to note that the BOLD signal at 2 months old, when animals are still normotensive, is much lower than observed in our previous work in healthy 7-month old rats.<sup>15</sup> A possible explanation for this is that vascular or signaling changes observed in SHRs may be genetic, and begin prior to the onset of hypertension. This is supported by evidence seen in human studies that suggests a hereditary component to neurovascular adaptive or pathological changes in hypertension.<sup>33</sup> However, to investigate this, further study comparing 2-month old SHRs with age matched Wistar Kyoto rats would be required. An alternative explanation may be that the rat somatosensory cortex is not yet fully developed before 6 months old, and Wistar Kyoto rats may exhibit the same low baseline. A study at 4.7T on Sprague-Dawley rats showed that the size of the active region in the somatosensory cortex only increased until post-natal day 20, after which activation patterns remained the same into young adulthood. Signal intensity did increase between these time points.<sup>34</sup> However, this study only observed one “adult” time point, while rats’ brains are still thought to be developing up to 6 months old,<sup>35</sup> and so observing age-matched Wistar Kyoto rats would be beneficial to investigate if the BOLD response does change in this strain prior to 6 months.

ASL for CBF quantification showed an increase in CBF from 4 months onward, with no change at 6 months. This suggests that approximately halfway through the development of chronic hypertension, cerebral autoregulation cannot compensate for the sustained increase in BP. In healthy animals, transient systemic BP increases are counteracted by mechanisms of cerebral autoregulation to prevent hyperperfusion, which can be damaging to the brain. The elevated CBF observed

here suggests that these mechanisms are less effective at this time point, either through inhibition of signaling, or through reduced sensitivity of remodeled vessels. This supports previous observations in rodents, in which two-photon microscopy in 40-week old SHRs showed a sustained increase in CBF.<sup>36</sup> However, these findings in SHRS contradict previous research in humans, in which autoregulation is shifted in hypertensive subjects to counteract the effect of hypertension. When studying cerebral autoregulation between normotensive and hypertensive subjects, CBF has been shown to be the same in both groups when measured at each group’s mean BP.<sup>2</sup> In the longer term, human studies have shown that CBF is reduced below baseline, due to thickening of vascular smooth muscle and collagen deposition in arteries and veins, which reduces lumen diameter and distensibility.<sup>3,37</sup> Whether this occurs in SHRs may require studying animals for 12 months or more.<sup>36</sup> If CBF remains high throughout the lifetime of SHRs, then an alternative model of hypertension may be more appropriate for future studies.<sup>5</sup>

No significant changes were seen in  $\Delta\text{Glu}$  at any time point. If synaptic activity or neuronal metabolism were affected by chronic hypertension, a decrease in glutamate would be expected. This would represent either a decrease in glutamate release, or a decrease in metabolic activity behind glutamate turnover.<sup>38</sup> Impairment of neurovascular coupling, reducing delivery of oxygen and glucose during neuronal activity, would be expected to reduce neuronal energy production,<sup>39</sup> which would reduce cellular processes, such as glutamate turnover. That a change in glutamate is not observed would suggest that the changes shown in BP, CBF, and vascular reactivity are not impairing neuronal metabolism or synaptic activity at this point. NAA levels, a marker for neuronal viability, also do not change, suggesting that neuronal death does not occur at this stage. While further study using longer fMRS scans is needed, as SNR using this method was suboptimal, preservation of glutamate turnover rate and synaptic activity at 6 months suggests that the neuronal damage and cognitive deficits develop more slowly than chronic hypertension. If further time points were investigated with improved SNR, the time point at which synaptic impairment and neuronal death begin might be determined, indicating the possibility of a window in which neuroprotective strategies may be of benefit in chronic hypertension.

This study shows a clear change in BOLD response to forepaw stimulation and resting CBF in SHRs as animals age and hypertension develops. CBF increases at 4 months and remains elevated at 6 months. The BOLD signal reveals that the number of active voxels in the S1FL region decreases significantly between 4 and 6 months, while the magnitude of the BOLD signal does not significantly change. This suggests that while cerebral autoregulation is impaired in the acute stage of hypertension, protective mechanisms are active, which preserve the BOLD response at this stage, and the BOLD response is only affected in the chronic stage as pathological changes occur, and that neuronal damage does not occur at this stage. It is important to note that an upward trend was observed in BOLD signal intensity over time. While it was not statistically significant in this study, if a larger cohort and/or longer study showed a significant increase in signal intensity, this would indicate a more complex effect of BP/CBF on neurovascular coupling. Additionally, glutamate change with activation became

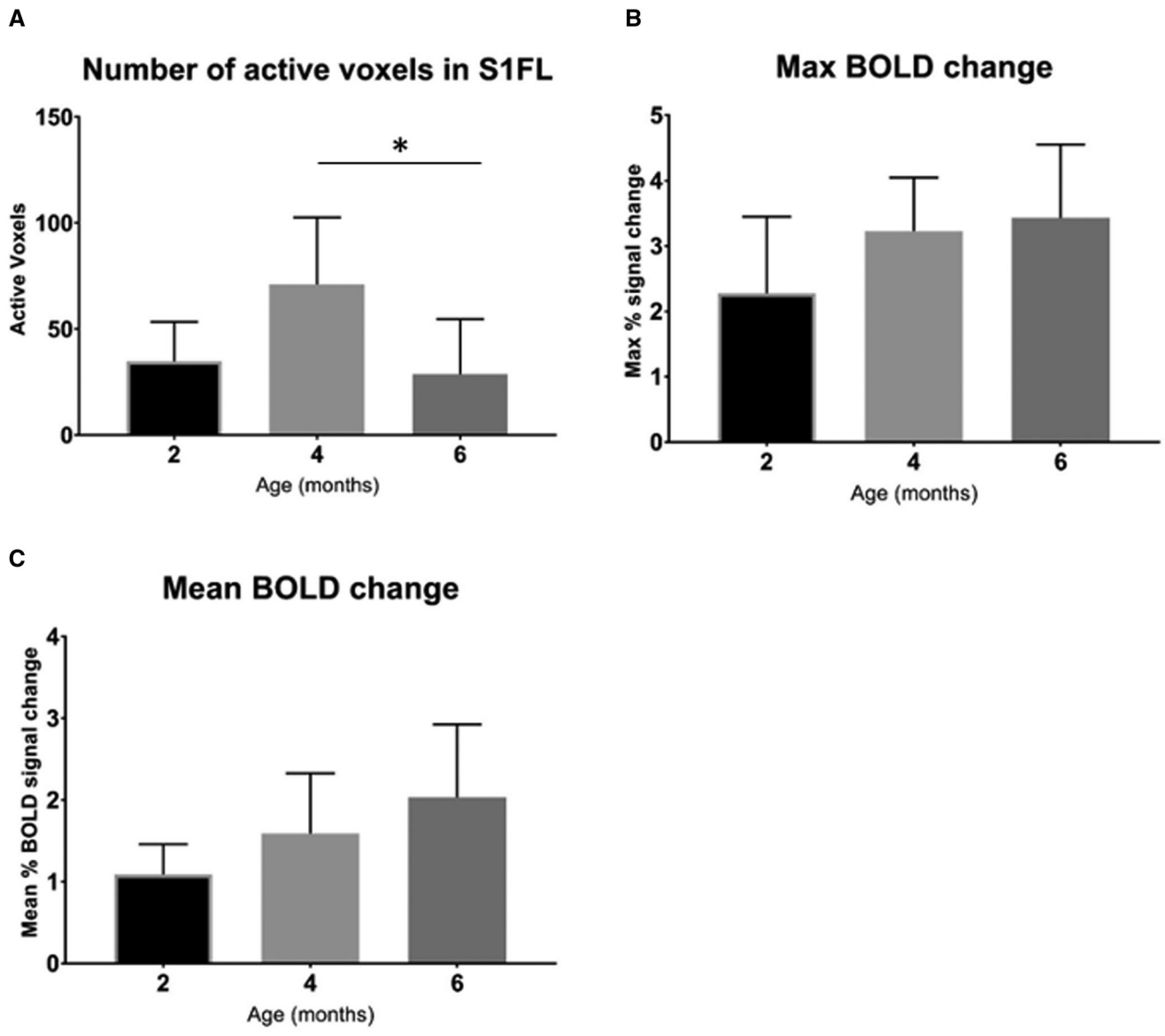


**Fig 3.** Bar graphs showing the number of active voxels in somatosensory cortex, forepaw region (S1FL) (A), maximum BOLD signal change in S1FL (B), and mean BOLD signal change of all active voxels in S1FL (C). Error bars indicate standard deviation. Lines marked \* indicate significant difference with  $P < .05$ . number of values = 6, 6, and 7 at 2, 4, and 6 months, respectively.

negative at later time points; however, this change was also not significant. Reduction of neurotransmitter turnover, combined with increased local BOLD response, would suggest an uncoupling of neuronal and vascular activity with chronic hypertension.

To our knowledge, this study is the first longitudinal fMRI study in hypertensive rats. This study does have the limitation of variable  $N$  between time points, due to technical issues with monitoring equipment in some scans. As this method had not previously been used in SHRs, we did not perform additional scans to account for missing data points, in order to minimize welfare risks from repeated anesthesia in a short time. This limitation can be rectified in a future study. In the current study, we only used female rats, to prevent any risk of fighting that may arise in longer term group housed males, and future studies are relevant to both males and females. A future study may

also require larger animal numbers, and the data here can be used in prospective power calculations. The methods, which were initially developed using a rat model of healthy aging,<sup>15</sup> were adapted for SHR physiology, as during the anesthetic testing prior to experiments, after cannulating the tail vein, the tail vein rapidly constricted and blocked the application of propofol. As this was observed before hypertension developed, this is likely an inherent trait of the SHR strain, similar to other inherited adaptive traits seen in humans with a family history of hypertension.<sup>33</sup> This was mitigated through application of lidocaine to the base of the tail, preventing the vein from constricting and allowing for 1 hour of propofol application before animals were returned to isoflurane. This may prevent longer scans from being performed, and so other scans may need to be removed to allow time for longer MRS scans in future experiments. It may also be feasible to use another model of

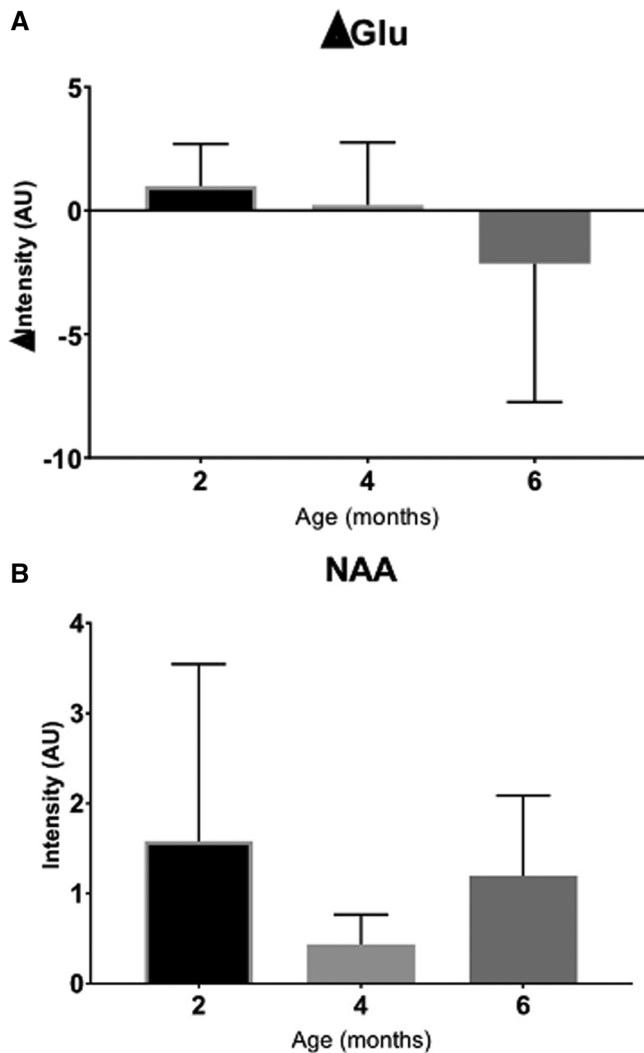


**Fig 4.** Glutamate (Glu) turnover in somatosensory cortex, forepaw region (A). N-acetyl aspartate (NAA) levels in somatosensory cortex over time (B). Error bars indicate standard deviation. Lines marked \* indicate significant difference with  $P < .05$  (A). number of values = 6, 8, and 7 at 2, 4, and 6 months, respectively.

hypertension, for example, salt and mineralocorticoid-induced hypertension in Wistar rats,<sup>5</sup> thus removing any hereditary factors that may be present in SHR, including, for example, the impact such factors may have on vein constriction. This would also allow the age of onset of hypertension to be determined by the researcher, rather than by the animals' genetics. However, the advantage of using SHR is that the progression of hypertension is well characterized and has low variability between animals. Inducing hypertension may have increased variability due to factors, such as human error, or stress on rats from the cumulative effect of multiple injections.<sup>5</sup> The noninvasive, multiparametric MRI protocol used here shows for the first time a link between BP, CBF, and BOLD signal in rats as hypertension progresses. Applying these methods to further study of SHR and other rodent models of hypertension could be beneficial in identifying how genetic and environmental factors in hypertensive subjects can affect brain health and function, and in the development of treatment for hypertension-related cognitive impairments.

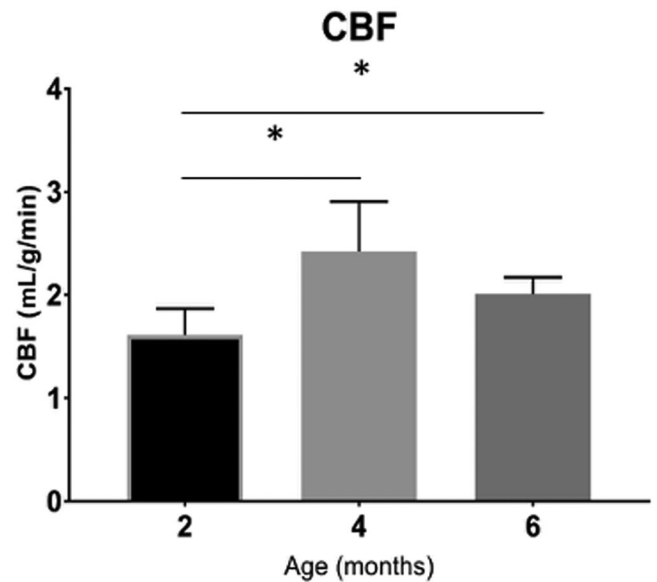


**Fig 5.** Resting CBF at bregma. Error bars indicate standard deviation. Lines marked \* indicate significant difference with  $P < .05$ . number of values = 7.

## References

- Cooper LL, Woodard T, Sigurdsson S, et al. Cerebrovascular damage mediates relations between aortic stiffness and memory. *Hypertension* 2016;67:176-82.
- Iadecola C, Gottesman RF. Neurovascular and cognitive dysfunction in hypertension. *Epidemiology, pathobiology and treatment. Circ Res* 2019;124:1025-44.
- Jennings JR, Muldoon MF, Ryan CM, et al. Cerebral blood flow in hypertensive patients, an initial report of reduced and compensatory blood flow responses during performance of two cognitive tasks. *Hypertension* 1998;31:1216-22.
- Thorin-Trescases N, de Montgolfier O, Pincon A, et al. Impact of pulse pressure on cerebrovascular events leading to age-related cognitive decline. *Am J Physiol Heart Circ Physiol* 2018;314:1214-24.
- Doggrell SA, Brown L. Rat models of hypertension, cardiac hypertrophy and failure. *Cardio Res* 1998;39:89-105.
- Heagerty AM, Aalkjaer C, Bund SJ, et al. Small artery structure in hypertension: dual processes of remodelling and growth. *Hypertension* 1993;21:392-7.
- Schiffin EL. Vascular remodelling in hypertension: mechanisms and treatment. *Hypertension* 2012;59:367-74.
- Waldenstein SR, Ryan CM, Polefrone JM, et al. Neuropsychological performance of young men who vary in familial risk for hypertension. *Psychosom Med* 1994;56:449-56.
- Schneider GM, Jacobs DW, Gevirtz RN, et al. Cardiovascular haemodynamic response to repeated mental stress in normotensive subjects at genetic risk of hypertension: evidence of enhanced reactivity, blunted adaptation, and delayed recovery. *J Hum Hypertens* 2003;17:829-40.
- Haley AP, Gunstad J, Cohen RA, et al. Neural correlates of visuospatial working memory in healthy young adults at risk for hypertension. *Brain Imaging Behav* 2008;2:192-9.
- Naumczyk P, Am S, Witkowska M, et al. Compensatory functional reorganization may precede hypertension-related brain damage and cognitive decline: a functional magnetic resonance imaging study. *J Hypertension* 2017;35:1252-62.
- Li X, Liang Y, Chen Y, et al. Disrupted frontoparietal network mediates white matter structure dysfunction associated with cognitive decline in hypertension patients. *J Neurosci* 2015;35:10015-24.
- Fujishima M, Ibayashi S, Fujii K, et al. Cerebral blood flow and brain function in hypertension. *Hypertens Res* 1995;18:111-7.

14. Adams MA, Bobik A, Korner PI. Differential development of vascular and cardiac hypertrophy in genetic hypertension: relation to sympathetic function. *Hypertension* 1989;14:191-202.
15. Crofts A, Trotman-Lucas M, Janus J, et al. A longitudinal, multi-parametric functional MRI study to determine age-related changes in the rodent brain. *Neuroimage* 2020;218:116796.
16. Kilkenny C, Browne W, Cuthill IC, et al. Animal research: reporting in vivo experiments: the ARRIVE guidelines. *Brit J Pharmacol* 2010;160:1577-9.
17. Griffin KM, Blau CW, Kelly ME, et al. Propofol allows precise quantitative arterial spin labelling functional magnetic resonance imaging in the rat. *Neuroimage* 2010;51:1395-404.
18. Hyder F, Behar KL, Martin MA, et al. Dynamic magnetic resonance imaging of the rat brain during forepaw stimulation. *J Cereb Blood Flow Metab* 1994;14:649-55.
19. Gruetter R. Automatic, localized in vivo adjustment of all first- and second-order shim coils. *Magn Reson Med* 1992;29:804-11.
20. Slotboom J, Mehlkopf AF, Bovee WMMJ. A single-shot localization pulse sequence suited for coils with inhomogenous RF fields using adiabatic slice-selective RF pulses. *J Magn Reson* 1991;95:396-404.
21. Tremoleda JL, Kerton A, Gsell W. Anaesthesia and physiological monitoring during in vivo imaging of laboratory rodents: considerations on experimental outcomes and animal welfare. *EJNMMI Res* 2012;2:44.
22. Smith SM, Jenkinson M, Woolrich MW, et al. Advances in functional and structural MR image analysis and implementation as FSL. *Neuroimage* 2004;23:208-19.
23. Jenkinson M, Bannister P, Brady M, et al. Improved optimization for the robust and accurate linear registration and motion correction of brain images. *Neuroimage* 2002;17:825-41.
24. Smith SM. Fast robust automated brain extraction. *Hum Brain Mapp* 2002;17:143-55.
25. Wood T, Lythgoe D, Williams S. rBET: making BET work for rodent brains. *Presented at the 21st Annual Meeting of the International Society for Magnetic Resonance in Medicine* 2013, April 2–26, Salt Lake City, USA.
26. Zhang Y, Brady M, Smith S. Segmentation of brain MR images through a hidden Markov random field model and the expectation-maximization algorithm. *IEEE Trans Med Imaging* 2001;20:45-57.
27. Beckmann CF, Smith SM. Probabilistic independent component analysis for functional magnetic resonance imaging. *IEEE Trans Med Imag* 2004;23:137-52.
28. Woolrich MW, Ripley BD, Brady M, et al. Temporal autocorrelation in univariate linear modeling of fMRI data. *Neuroimage* 2001;14:1370-86.
29. Baumann S, Griffiths TD, Rees A, et al. Characterisation of the BOLD response time course at different levels of the auditory pathway in non-human primates. *Neuroimage* 2010;50:1099-108.
30. Simpson R, Devenyi GA, Jezzard P, et al. Advanced processing and simulation of MRS data using the FID appliance (FID-A) – an open source MATLAB-based toolkit. *Magn Reson Med* 2017;77:23-33.
31. Williams DS, Detre JA, Leigh JS, et al. Magnetic resonance imaging of perfusion using spin inversion of arterial water. *Proc Natl Acad Sci USA* 1992;89:212-6.
32. Mori S, Kato M, Fuhishima M. Impaired maze learning and cerebral glucose utilization in aged hypertensive rats. *Hypertension* 1995;25:545-53.
33. Haley AP, Sweet LH, Gunstad J, et al. Verbal working memory and atherosclerosis in patients with cardiovascular disease: an fMRI study. *J Neuroimaging* 2007;17:227-33.
34. Colonnese MT, Phillips MA, Constantine-Paton M, et al. Development of hemodynamic responses and functional connectivity in rat somatosensory cortex. *Nat Neurosci* 2008;11:72-9.
35. Sengupta P. The laboratory rat: relating its age with humans. *Int J Preventative Med* 2013;4:624-30.
36. Calcinaghi N, Wyss MT, Jolivet R, et al. Multimodal imaging in rats reveals impaired neurovascular coupling in sustained hypertension. *Stroke* 2013;44:1957-64.
37. Sciffin EL. Vascular stiffening and arterial compliance: implications for systolic blood pressure. *Am J Hypertens* 2004;17:39-48.
38. Walls AB, Waagpetersen HS, Bak LK, et al. The glutamine-glutamate/GABA cycle: function, regional differences in glutamate and GABA production and effects of interference with GABA metabolism. *Neurochem Res* 2015;40:402-9.
39. Stanimirovic DB, Friedman A. Pathophysiology of the neurovascular unit: disease cause or consequence? *J Cereb Blood Flow Metab* 2012;32:1207-21.